Propagation of the Hawaiian-Emperor volcano chain by Pacific plate cooling stress

W. D. Stuart
US Geological Survey, Menlo Park, CA 94025, USA

G. R. Foulger
Department of Earth Sciences, Durham University, Durham DH1 3LE, UK

M. Barall
US Geological Survey, Menlo Park, CA 94025, USA

ABSTRACT

The lithosphere crack model, the main alternative to the mantle plume model for age-progressive magma emplacement along the Hawaiian-Emperor volcano chain, requires the maximum horizontal tensile stress to be normal to the volcano chain. However, published stress fields calculated from Pacific lithosphere tractions and body forces (e.g., subduction pull, basal drag, lithosphere density) are not optimal for southeast propagation of a stress-free, vertical, tensile crack coincident with the Hawaiian segment of the Hawaiian-Emperor chain. Here we calculate the thermoelastic stress rate for present-day cooling of the Pacific plate using a spherical shell finite element representation of the plate geometry. We use observed seafloor isochrons and a standard model for lithosphere cooling to specify the time dependence of vertical temperature profiles. The calculated stress rate multiplied by a time increment (e.g., 1 Ma) then gives a thermoelastic stress increment for the evolving Pacific plate. Near the Hawaiian chain position, the calculated stress increment in the lower part of the shell is extensional with maximum extension normal to the chain direction. Near the projection of the chain trend to the southeast beyond Hawaii, the stress increment is compressive. This incremental stress field, if the main contribution to the total Pacific plate stress field, could produce a tensile crack or similar propagating flaw model for the Hawaiian volcano chain.

INTRODUCTION

The two main explanations for the Hawaiian-Emperor volcano chain are mantle plume models (Morgan, 1971; Sleep, 1992) and lithosphere propagating crack models (Dana, 1849; Jackson and Shaw, 1975; Clague and Dalrymple, 1989). Both require northwest motion of the Pacific plate with respect to Hawaii (Fig. 1). In plume models, the plume top is the magma source, and the observed age-progressive sequence of volcanoes is produced by a buoyant plume column that is fixed with respect to the deep mantle. In crack models, a vertical tensile crack through the lithosphere coincides with the Hawaiian volcano chain, and magma is produced by decompression melting at depth near the crack-tip stress concentration, currently at Hawaii. The location of this stress concentration depends on the plate-wide stress field, which in turn is controlled by tractions and body forces acting on the plate as a whole. Since such a stress field is approximately stationary with respect to the boundary around the entire circumference of the plate, it follows that the chain of progressively older volcanoes to the northwest results from motion of Pacific plate material relative to the plate's evolving boundary. In other words, the preferred reference frame for Pacific plate motion is not the mantle, but is instead the slowly changing boundary of the Pacific plate

Propagating crack models for the Hawaiian chain have not, to date, been developed beyond qualitative form, but one can infer the symmetry that the model's driving stress field must have. If the presently propagating crack lacks shear strength, cuts the entire lithosphere, and coincides with part or all of the Hawaiian chain, then the chain straightness implies the existence of a plate stress field symmetric to the crack plane in its neighborhood. This is because such a tensile crack propagates in its own plane under this condition. (In fact, neither the Hawaiian nor the Emperor chain is exactly straight on a small scale, and the Hawaiian chain has changed propagation direction in the last few Ma (Wessel and Kroenke, 2000).) Chain straightness also implies that the crack is nearly parallel to the Pacific plate velocity vector with respect to its boundary, otherwise older portions of the active crack would be carried into unfavorable areas of the stress field. Finally, the southeast crack tip would be near the location where crack-normal stress vanishes or becomes compressive.

Solomon and Sleep (1974) and Sandwell et al. (1995) suggested, using a symmetry argument, that the opposed pulls of subducted slabs under the Aleutian Islands and in the southwest Pacific could induce maximum horizontal tension perpendicular to the Hawaiian chain near the chain. However, global or Pacific plate models where lithosphere stress is calculated from tractions and gravity body forces (Richardson et al., 1979; Wortel et al., 1991; Bai et al., 1992; Steinberger et al., 2001; Yoshida et al., 2001; Lithgow-Bertelloni and Guynn; 2004) generally have horizontal stress unfavorable to the crack model. The stress models either lack maximum tension along and normal to the Hawaiian chain, or they have tensile stress along the southeast projection of the chain, ahead of the present position of Hawaii. In some cases the model stress fields seem to be too spatially variable to support a simple crack model. Perhaps the computed stress fields most consistent with a crack model are Lithgow-Bertelloni and Guynn (2004) cases TD0 and TD5, which are based on lateral heterogeneity of the lithosphere.

In this paper we calculate the present stress rate field due to cooling of the

Pacific plate as it moves away from the East Pacific Rise. In contrast to these earlier studies of slab pull, we find that the horizontal stress rate field near the Hawaiian segment from this thermal source has symmetry and sign favorable to lithosphere crack models.

THERMOELASTIC STRESS FIELD

The present-day total thermoelastic stress field cannot be calculated directly from only current Pacific plate properties because the plate has unknown initial conditions and an unknown history of cooling, accretion at its base and ridge boundaries, and ablation at subduction zones. Instead, we calculate the present instantaneous time derivative of stress at particle positions. However, our subsequent discussion is perhaps more intuitive when expressed in terms of stress, so we multiply our computed stress rate by 1 Ma to obtain a stress increment whose numerical value is the same as that of the stress rate. This stress increment is an approximation to the true thermoelastic stress increment that would be obtained by allowing the plate geometry to change slightly during the passage of 1 Ma.

First, we represent the Pacific plate as a finite-element spherical shell (in spherical coordinates) where elements are elastic and the shell lateral boundary approximates the actual plate boundary as shown in Fig. 1. Then, we assign to each element the temperature derivative with respect to time determined from a standard analytic equation for vertical conductive heat transfer in a cooling half-space (Turcotte and Schubert, 2002) according to seafloor age interpolated from seafloor isochron lines (Mueller et al., 1997) (Fig. 1). The bottom boundary of the elastic plate is defined to be at the 800˚C isotherm as calculated from the above equation. When the 800˚C isotherm corresponds to depths > 50 km (i.e., plate older than 50 Ma), we assign the shell depth to be 50 km. The 50-km maximum depth is a compromise between depths estimated two ways. With respect to the passage of seismic waves, the Pacific plate lithosphere attains a steady-state thickness of 80-100 km for lithosphere older than about 100 Ma (Turcotte and Schubert, 2002; Watts, 2001). Also, the depth of low-density compensation for the Hawaiian swell (discussed below) is about 100 km (Turcotte and Schubert, 2002). On the other hand, the elastic flexural thickness of the lithosphere near Hawaiian-Emperor volcanoes is 20-30 km (Watts, 2001). For global oceanic lithosphere older than ~70 Ma, cooling of a 95-km thick plate with basal temperature 1450˚C is more consistent with heat flow and seafloor depth data than a half-space model (Stein and Stein, 1992). Our result is an approximation to the solution of a more realistic cooling problem where the upper part of the lithosphere would be elastic and the lower part would become more anelastic with depth.

The shell has 62,192 3D quadratic elements (not membrane) and is divided into four layers of equal thickness vertically but variable thickness horizontally. Thermal diffusivity is 8×10^{-7} m^2 s^{-1}; volume coefficient of thermal expansion, 3.1×10^{-5} ˚C^{-1}; initial temperature, 1300˚C; Poisson's ratio, 0.25; and shear modulus, 30 GPa. Boundary conditions are zero traction on all surfaces, zero radial displacement at the shell bottom, and a minimal displacement constraint to prevent rigid motion. More pervasive displacement boundary conditions are not appropriate because over geologic time all parts of the Pacific plate move with respect to surrounding plates. We did not study the consequences of replacing the zero vertical displacement

condition at the shell bottom with a force condition to simulate isostatic equilibrium.

Figs. 2 and 3 show principal stress vectors and mean normal stress for the calculated 1 Ma increment of horizontal stress for shell layers 2 and 4 (bottom). In layer 2 (Fig. 2) near the East Pacific Rise and the Juan de Fuca ridge (Fig. 1), rapid thermal contraction produces strong tensile stress. This strong contraction in turn compresses the adjacent shell material on the left to about the middle of the plate. From there to the subduction zones the stress field becomes more tensional. The west half of the Hawaiian chain has slight tension normal to the chain. The Louisville chain has tension near its two ends, and compression along its center. Stresses are compressive near the Marquesas, Pitcairn, and Society chains of the south Pacific superswell area. Layer 4 (Fig. 3) is similar except that the stress field is overall more tensional. The prominent tensional region near Samoa, caused by a notch in the Pacific plate boundary, occurs in all layers. Principal stresses in the interior of layer 1 (not shown) are orientated similar to those in layer 2 but are compressive except near Samoa, near the plate boundary notch at the east end of the Louisville chain, in a small area adjacent to the southern-most East Pacific Rise, and in a small area adjacent to the Juan de Fuca ridge. In a depth-averaged sense, one may think of thermal contraction along part of the shell rim as stretching the rest of the shell rim. At a particular horizontal location away from a ridge, however, thermal contraction at the plate bottom produces tensile stress near the plate bottom and compressive stress near the top.

DISCUSSION

Thermoelastic Stress Field

The Hawaiian chain is qualitatively consistent in direction and length with the crack model if the plate stress is predominantly thermoelastic and the incremental thermoelastic stress and the unknown total thermoelastic stress have similar form. Near the Hawaiian volcano chain the incremental stress in layers 2-4 (Figs. 2 and 3) is nearly symmetric with respect to the chain, with principal tension normal to the chain and principal compression parallel to it. Of all straight trial cracks that can be drawn on Figs. 2 and 3, cracks close to the Hawaiian line are the longest that have principal tension normal to them over their full length. The Hawaiian line is also parallel to Pacific plate motion (relative to its ridge boundary), and so straight cracks close to the Hawaiian line stay in a favorable stress field for the longest time. On a southeast extrapolation of the Hawaiian line, principal stresses become compressive and rotate clockwise and thus may explain the location of the Hawaiian hotspot as the position beyond which an equilibrium straight crack cannot propagate under the applied plate stress. The Louisville chain, like the Hawaiian-Emperor chain, is age-progressive east-to-west (Clouard and Bonneville, 2005). On Figs. 2 and 3, the maximum tensile stress at the east end of the Louisville chain, near the East Pacific Rise, is oriented approximately normal to the volcano chain, consistent with a tensile crack theory for the chain end. On the other hand, principal stress directions near the east-to-west age-progressive Marquesas, Pitcairn, and Society chains (Clouard and Bonneville, 2005) are inconsistent with a simple crack theory.

If calculated thermoelastic stress rates are applied for a 10 Ma time interval,

the magnitudes of thermoelastic tensile stresses in layer 4 normal to and near the Hawaiian chain for 10 Ma are about 10 MPa. Their magnitude is then comparable to tensional stresses for the two favorable cases of Lithgow-Bertelloni and Guynn (2004) for the region near the Hawaiian chain. Stress magnitudes near the Hawaiian chain for other plate models are quite variable, but are usually less than about 100 MPa.

Since the incremental stress field by itself makes the crack model consistent with the observed Hawaiian chain, the superposition of actual stresses from all other sources must resemble the incremental form for a crack model to apply. The possibilities are (1) non-thermoelastic stresses are negligible, and total and incremental thermoelastic stresses have the same form, (2) non-thermoelastic stresses are not negligible, but combine in a fortuitous way with the total thermoelastic stress to have the necessary form. A special case of (2) is that non-thermoelastic stresses, total thermoelastic, and incremental thermoelastic stress all have the same form. Conversely, a crack model independently known to be correct and driven by a known total thermoelastic stress places bounds on plate tractions and body forces.

For a long-term stable plate boundary configuration (and this has probably persisted since as long ago as Late Oligocene), the current total thermoelastic stress would be approximately equal to the sum of incremental stresses, allowing for motion of plate material with respect to the boundary, calculated over time. Thus the total and incremental stress fields would have nearly the same symmetry with respect to the Hawaiian line, but the position of stress sign reversal along the Hawaiian line is uncertain.

Emperor Chain, Hawaiian-Emperor Bend, Hawaiian Swell

If the above stress rate results are a good approximation to the actual total stress field, Figs. 2 and 3 imply that the Emperor chain is not a propagating tensile crack in a thermoelastic stress field at present because the direction of maximum tension is inclined to the crack plane. From about 80 Ma to 47 Ma, the age of the Hawaiian-Emperor bend (Tarduno et al., 2003), the Pacific plate was much smaller than it is today and had ridge boundaries on the north (Pacific-Kula), east (Pacific-Farallon), and southwest (Pacific-North New Guinea) (Smith, 2003, this volume; Hall, 1997). The Emperor chain is thought to have originated at the Pacific-Kula / Izanagi ridge axis as a result of excess volcanism associated with a 30˚ change in spreading direction from 84 to 71 Ma (Norton, this volume). This volcanism built the Meiji seamount, the oldest in the Emperor chain. One explanation for the Emperor chain is that it was a crack near the Kula ridge that propagated southeastward until the ridge became inactive around 47 Ma. A simple mechanical history for the Hawaiian-Emperor crack would then be that the Emperor chain propagated first inside the Pacific-Kula ridge thermal boundary layer and then near 47 Ma found itself in the outer field of the East Pacific Rise thermal boundary layer. In other words, the cause of the Hawaiian-Emperor bend may be a rapid change in the thermoelastic stress field associated with the disappearance of ridge segments. In a thermoelastic stress field, no fixed latitude is necessarily implied for Emperor chain volcanoes, but the observed latitude decrease with time (Tarduno et al., 2003; Sager, this volume) has yet to be simulated in an evolving thermoelastic crack model. On the other hand, the observed bend of the Hawaiian-Emperor chain appears not to correspond to an appropriate change in Pacific plate motion (Norton, 1995).

The Hawaiian swell, a region of elevated seafloor ~1200 km wide, ~2500 km long, and coincident with the younger half of the Hawaiian chain (Fig. 1), has been attributed to (1) a thermal source (Crough, 1983), and (2) buoyant residuum left behind from melt extraction and underplated onto the base of the lithosphere, spreading viscously with time (Phipps Morgan et al., 1995). A thermal anomaly along the swell has not been observed (von Herzen et al., 1989). It has been suggested that its absence may be due to hydrothermal circulation (McNutt, 2002), but DeLaughter et al. (2005) and Stein and von Herzen (this volume) suggest that hydrothermal circulation is unlikely to be able to camouflage the heatflow anomalies expected from thermal plumes. Crack models attribute the swell to model (2), i.e., buoyant residuum, a theory that is supported by the observation that the volume of the swell is roughly proportional to the volume of melt extracted along the chain (Phipps Morgan et al., 1995).

CONCLUDING REMARKS

The present work represents a first step towards quantifying the crack model that was suggested for the Hawaiian volcanic chain as far back as Dana (1849). The crack model is appealing because several first-order features of the Hawaiian and Emperor chains that are inconsistent with the plume model or require surprising coincidences may be consistent with the crack model. These include the inception of the Emperor chain on a ridge, the lack of a "plume head" large igneous province (LIP), the ~ 60˚ change in propagation direction that occurred at ~ 47 Ma, the rapid southward migration of the Emperor hot spot prior to this, and the lack of the heatflow anomaly expected for a plume.

Nevertheless, current lithosphere crack models are difficult to test. There are no solved boundary value problems available to study conditions for crack propagation, melt production, and melt transport, and in particular, the spatial extent of the crack or equivalent lithosphere flaw is unknown. Neither is it clear, given current technology, how the very small extension rates expected at the surface above a crack could be measured geodetically in the Hawaii region. Further numerical modeling is needed to evaluate the present initial results and to make predictions that are capable of being tested using presently available methods.

ACKNOWLEDGEMENTS

We thank D. Anderson, J. Moore, J. Savage N. Sleep, S. Stein and D. Jurdy (editor) for helpful suggestions that improved the manuscript.

REFERENCES CITED

Bai, W., Vigny, C., Ricard, Y., and Froidevaux, C., 1992, On the origin of deviatoric stresses in the lithosphere: Journal of Geophysical Research, v. 97, p. 11,729-11,737.

Clague, D. D., and Dalrymple, G. B., 1989, Tectonics, geochronolgy, and origin of the Hawaiian-Emperor volcanic chain, in Decker, R. W., ed., Boulder, Colorado, Geological Society of America, Geology of North America, v. N, p. 188-217.

Clouard, V., and Bonneville, A., 2005, Ages of seamounts, islands, and plateaus on the Pacific plate, in Foulger, G. R., Natland, J. H., Presnall, D. C., and Anderson, D. L., eds., Plates, plumes, and paradigms: Geological Society of America Special Paper 388, p. 71-90, doi: 10.1130/2005.2388(06).

Crough, S. T., 1983, Hotspot swells: Annual Review of Earth and Planetary Sciences , v. 11, p. 165-193.

Dana, J.D., 1849, U.S. Exploring Expedition during the years 1838-1842 under the command of Charles Wilkes, U.S.N., Geology, v. 10, p. 307-336.

DeLaughter, J. E., Stein, C. A., and Stein, S., 2005, Hotspots: A view from the swells, in Foulger, G. R., Natland, J. H., Presnall, D. C., and Anderson, D. L., eds., Plates, plumes, and paradigms: Geological Society of America Special Paper 388, p. 257-278, doi: 10.1130/2005.2388(16).

Hall, R., 1997, Cenozoic plate tectonic reconstructions of SE Asia, in Fraser, A. J., Matthews, S. J., and Murphy, R. W., eds., Petroleum Geology of Southeast Asia: Geological Society of London, Spec. Publ. No. 126, p. 11-23.

Jackson, E. D., and Shaw, H. R., 1975, Stress fields in central portions of the Pacific plate: Delineated in time by linear volcanic chains: Journal of Geophysical Research, v. 80, p. 1861-1874.

Lithgow-Bertelloni, C., and Guynn, J. H., 2004, Origin of the lithospheric stress field: Journal of Geophysical Research, v. 109, B01408, doi:10,1029/2003JB002467.

McNutt, M., 2002, Heat flow variations over Hawaiian swell controlled by near-surface processes, not plume properties, in Takahashi, E., Lipman, P. W., Garcia, M. O., Naka, J., and Aramaki, S., eds., Hawaiian volcanoes: Deep underwater perspectives: American Geophysical Union, Geophysical Monograph Series, v. 128, p. 365-372.

Morgan, W. J., 1971, Convection plumes in the lower mantle: Nature, v. 230, p. 42-43.

Mueller, R. D., Roest, W. R., Royer, J.-Y., Gahagan, L. M., and Sclater, J. G., 1997, Digital isochrons of the worldís ocean floor: Journal of Geophysical Research, v. 102, p. 3211-3214.

Norton, I. O., 1995, Plate motions in the North Pacific: The 43 Ma nonevent:

Tectonics, v. 14, p. 1080-1094.

Norton, I. O., 2006, Speculations on Cretaceous tectonic history of the Northwest Pacific and a tectonic origin for the Hawaii hotspot, in Foulger, G. R., and Jurdy, D. M., eds., Plates, plumes, and planetary processes: Geological Society of America Special Paper, this volume.

Phipps Morgan, J., Morgan, W. J., and Price, E., 1995, Hotspot melting generates both hotspot volcanism and a hotspot swell?: Journal of Geophysical Research, v. 100, p. 8045-8062.

Richardson, R.M., Solomon, S. C., and Sleep, N. H., 1979, Tectonic stress in the plates: Reviews of Geophysics, v. 17, p. 981-1019.

Sager, W. W., Divergence between paleomagnetic and hotspot model predicted polar wander for the Pacific plate with implications for hotspot fixity, Plates, plumes, and planetary processes: Geological Society of America Special Paper, this volume.

Sandwell, D. T., Winterer, E. L., Mammerickx, J., Duncan, R. A., Lynch, M. A., Levitt, D. A., and Johnson, C. L., 1995, Evidence for diffuse extension of the Pacific plate from Pukapuka ridges and cross-grain gravity lineations: Journal of Geophysical Research, v. 100, p. 15,087-15,099.

Simkin, T., Tilling, R. I., Vogt, P. R., Kirby, S., Kimberly, P., and Stewart, D. B., 2006, This dynamic planet: World map of volcanoes, earthquakes, impact craters, and plate tectonics: U.S. Geological Survey, Geologic Investigations Series Map I-2800.

Sleep, N. H., 1992, Hotspot volcanism and mantle plumes: Annual Review of Earth and Planetary Sciences, v. 20, p. 19-43.

Smith, A. D., 2003, A re-appraisal of stress field and convective roll models for the origin and distribution of Cretaceous to Recent intraplate volcanism in the Pacific basin: International Geology Review, v. 45, p. 287-302.

Smith, A. D., A shallow-source plate model for intraplate volcanism in the Panthalassan and Pacific Ocean basins, Plates, plumes, and planetary processes: Geological Society of America Special Paper, this volume.

Solomon, S. C., and Sleep, N. H., 1974, Some simple physical models for absolute plate motions: Journal of Geophysical Research, v. 79, p. 2557-2567.

Stein, C. A., and Stein, S. A., 1992, A model for the global variation in oceanic depth and heat-flow with lithospheric age: Nature, v. 359, p. 123-129.

Stein, Carol A., andVon Herzen, R. P., Geothermics of hotspot swells: Potential effects of hydrothermal circulation and magmatism, Plates, plumes, and planetary processes: Geological Society of America Special Paper, this volume.

Steinberger, B., H. Schmeling, and Marquart, G., 2001, Large-scale lithospheric stress field and topography induced by global mantle circulation: Earth and Planetary

Science Letters, v. 186, p. 75-91.

Tarduno, J. A., Duncan, R. A., Scholl, D. W., Cottrell, R. D., Steinberger, B., Thordarson, T., Kerr, B. C., Neal, C. R., Frey, F. A., Torii, M., and Carvallo, C., 2003, The Emperor seamounts: Southward motion of the Hawaiian hotspot plume in Earth's mantle: Science, v. 301, p. 1064-1069.

Turcotte, D. L., and Schubert, G., 2002, Geodynamics: 2nd ed., New York, Cambridge Univ. Press, 456 p.

von Herzen, R. P., Cordery, M. J., Detrick, R. S., and Fang, C., 1989, Heat-flow and the thermal origin of hot spot swells -- the Hawaiian swell revisited: Journal of Geophysical Research, v. 94, p. 13,783-13,799.

Watts, A. B., 2001, Isostasy and flexure of the lithosphere: New York, Cambridge Univ. Press, 458 p.

Wessel, P., and Kroenke, L. W., 2000, Ontong Java Plateau and late Neogene changes in Pacific plate motion: Journal of Geophysical Research, v. 105, p. 28,255-28,277.

Wortel, M. J. R., Remkes, M. J. N., Govers, R., Cloetingh, S. A. P. L., and Meijer, P. Th., 1991, Dynamics of the lithosphere and the intraplate stress field: Royal Society of London Philosophical Transactions, ser. A, v. 337, p. 111-126.

Yoshida, M., Honda, S., Kido, M., and Iwase, Y., 2001, Numerical simulation for the prediction of the plate motions: Effects of lateral viscosity variations in the lithosphere: Earth, Planets and Space, v. 53, p. 709-721.

FIGURE CAPTIONS

Figure 1: Bathymetry and topography of the Pacific seafloor and surrounding area (Simkin et al., 2006). Seafloor age (Mueller et al., 1997) is shown by isochron lines labeled in Ma. Continuous black line is boundary of elastic shell approximation to the Pacific plate as shown in Figs. 2 and 3. Continuous red lines near the model boundary are the present-day spreading East Pacific Rise and Juan de Fuca ridge (JDF). Hawaiian swell is light blue and has ~ 1 km maximum elevation above surrounding seafloor. Volcano chains shown are Hawaiian-Emperor; Louisville, L; Marquesas, M; Pitcairn, P; Society, S; and Samoa, Sa. Me is Meiji seamount.

Figure 2: Calculated increment of horizontal stress field for the Pacific plate for the second finite element layer from the top for 1 Ma. Horizontal principal stress vectors are shown by orthogonal line pairs, thin lines for tension, thick lines for compression. Principal stress vectors greater than 10 MPa are not shown. Magnitude of horizontal mean normal stress is shown by color, with maximum tension bright red and maximum compression bright blue; magnitudes greater than 5 MPa are plotted as 5 MPa. Green lines are the volcano chains marked in Fig. 1. Abbreviations as for Fig. 1.

Figure 3: Same as figure 2 but increment of horizontal stress field for the bottom layer is shown.

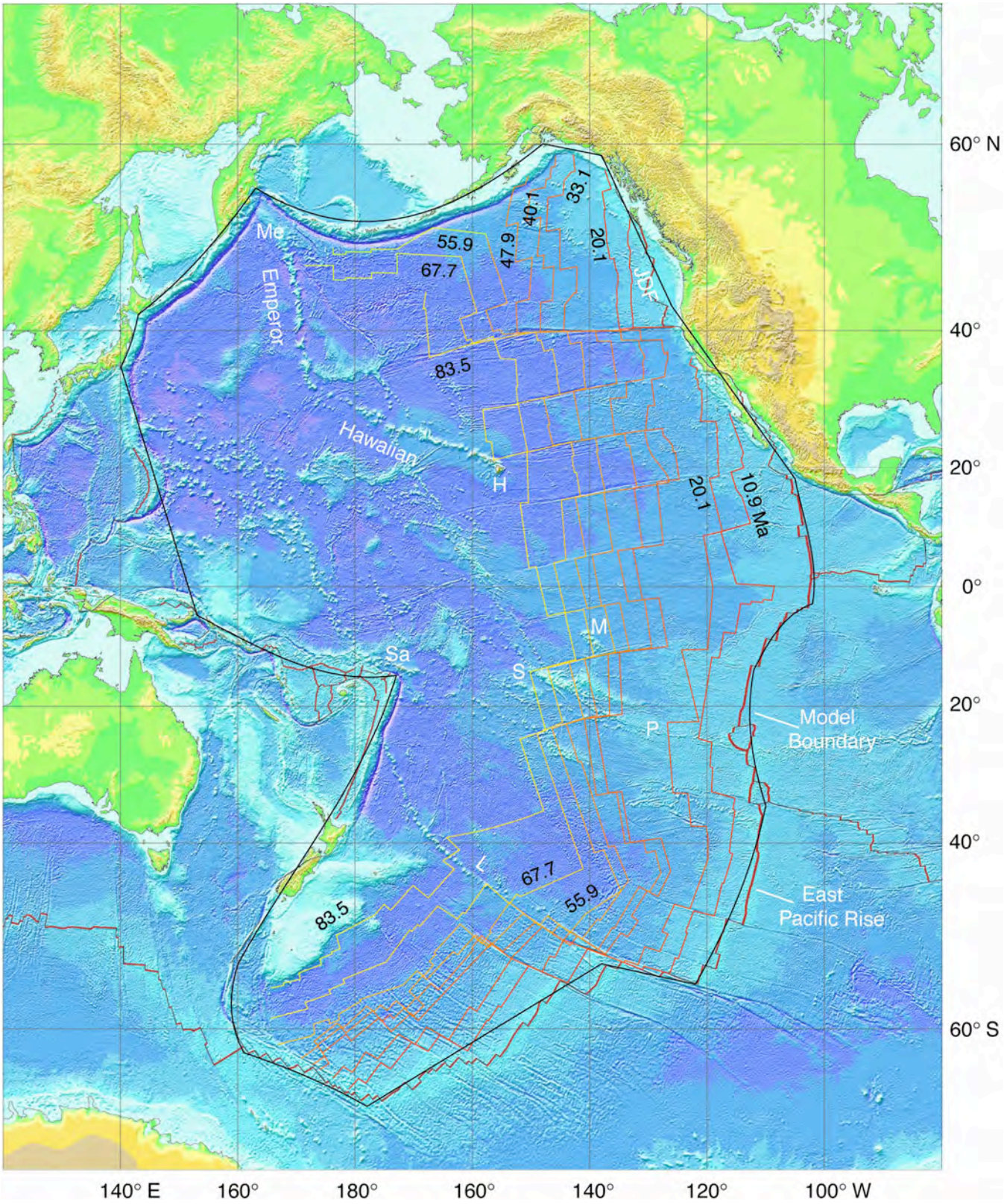
60° N
40°
20°
0°
20°
40°
60° S
140° E
160°
180°
160°
140°
120°
100° W
Me
Emperor
Hawaiian
55.9
67.7
83.5
47.9
40.1
33.1
20.1
JDF
20.1
10.9 Ma
H
M
S
Sa
P
L
67.7
55.9
83.5
Model
Boundary
East
Pacific Rise

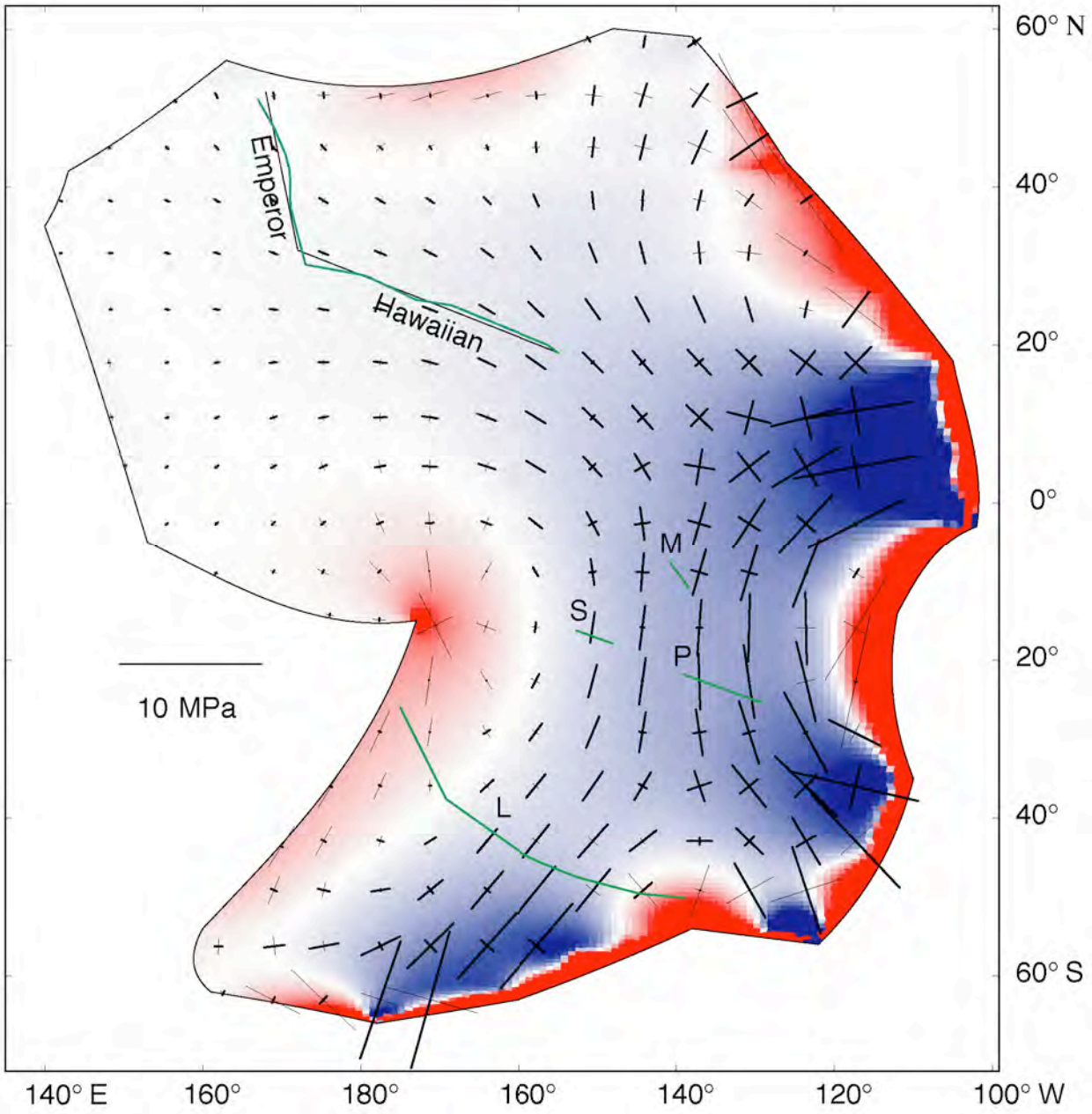
Emperor
Hawaiian
M
S
P
L
10 MPa
60° N
40°
20°
0°
20°
40°
60° S
140° E
160°
180°
160°
140°
120°
100° W

Fig. 2

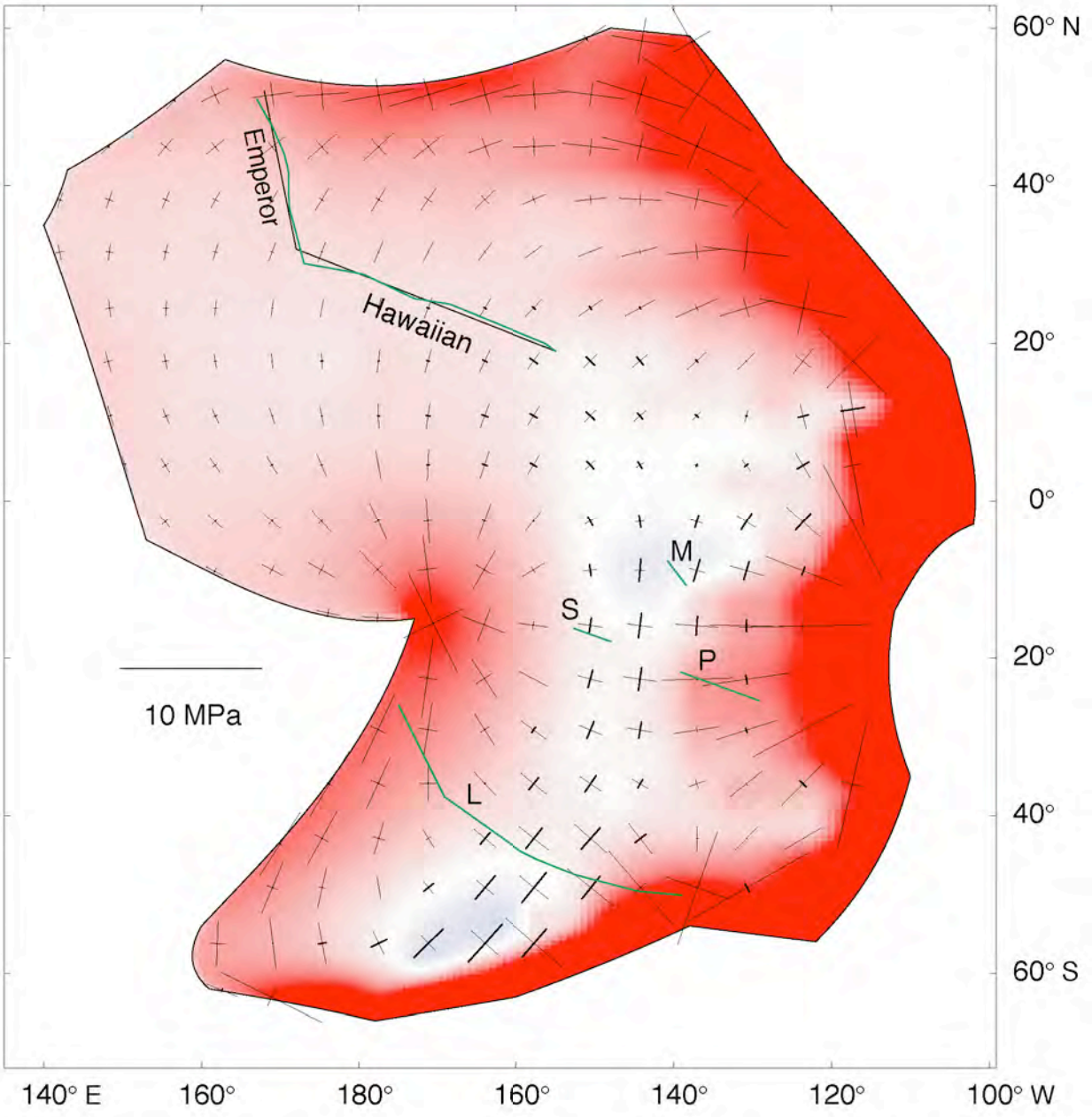
Emperor
Hawaiian
M
S
P
L
10 MPa
60° N
40°
20°
0°
20°
40°
60° S
140° E
160°
180°
160°
140°
120°
100° W

Fig. 3